arXiv:1608.04082v1 [cs.GR] 14 Aug 2016

# A weighted binary average of point-normal pairs with application to subdivision schemes

Evgeny Lipovetsky*,† Nira Dyn‡

**Abstract**

Subdivision is a well-known and established method for generating smooth curves and surfaces from discrete data by repeated refinements. The typical input for such a process is a mesh of vertices. In this work we propose to refine 2D data consisting of vertices of a polygon and a normal at each vertex. Our core refinement procedure is based on a ***circle average***, which is a new non-linear weighted average of two points and their corresponding normals. The ability to locally approximate curves by the circle average is demonstrated. With this ability, the circle average is a candidate for modifying linear subdivision schemes refining points, to schemes refining point-normal pairs. This is done by replacing the weighted binary arithmetic means in a linear subdivision scheme, expressed in terms of repeated binary averages, by circle averages with the same weights. Here we investigate the modified Lane-Riesenfeld algorithm and the 4-point scheme. For the case that the initial data consists of a control polygon only, a naive method for choosing initial normals is proposed. An example demonstrates the superiority of the above two modified schemes, with the naive choice of initial normals over the corresponding linear schemes, when applied to a control polygon with edges of significantly different lengths.

**Keywords:** non-linear subdivision schemes, 2D curve design, weighted binary average of point-normal pairs, convergence, Lane-Riesenfeld algorithm, 4-point scheme

## 1 Introduction

Subdivision schemes generate smooth curves/surfaces from discrete data by repeated refinements. Linear schemes are well understood and have been used in applications, such as Computer Graphics and Computer Aided Geometric Design. The typical input to these schemes consists of a mesh of vertices. For information on linear subdivision schemes see e.g. [9]. In recent years linear schemes were adapted to refine other types of geometric objects such as sets, manifold-valued data, and nets of functions (see e.g. [7], [15], [16], [4]).

This paper is motivated by the idea to design subdivision schemes generating surfaces by repeated refinements of 3D point-normal pairs. As a first step

*Corresponding author
†evgenyl@post.tau.ac.il, School of Computer Sciences, Tel-Aviv Univ.,Israel
‡niradyn@post.tau.ac.il, School of Mathematical Sciences, Tel-Aviv Univ., Israel

towards this aim we designed and investigated subdivision schemes generating 2D curves by repeated refinements of 2D point-normal pairs (PNPs). The subdivision schemes considered in this work are based on a geometric construction. These schemes are significantly different from Hermite schemes, which are linear schemes refining point-tangent pairs [14]. We plan to extend our schemes to schemes generating surfaces by refining point-normal pairs. It is important to note that point-normal pairs can be obtained from point-tangent pairs but not vice-versa.

The approach taken here is similar to that taken in the adaptation of linear subdivision schemes to manifold-valued data in [11],[16] and to sets in [7],[12]. The binary arithmetic mean in the refinement rules of linear subdivision schemes, expressed in terms of such repeated averages, is replaced by a weighted binary average of two PNPs. Such an average is designed here, based on a geometric construction involving a circle and hence its name *circle average*. With this average we modify the Lane-Riesenfeld algorithm [13], namely all spline subdivision schemes, and the 4-point scheme [5], [8] to refine PNPs.

Other modifications of these schemes which refine points are available. The most relevant to our work are [6],[1], and we plan to compare the performance of our modifications with their performance.

An interpolatory scheme refining PNPs, where the inserted PNP is determined by a similar construction to the circle average with weight $\frac{1}{2}$, is presented in [2]. While in [2], the scheme converges and the limit of the normals is equal to the normals of the limit curve, in our schemes this is not necessarily the case. Yet our approach yields a variety of subdivision schemes which are not limited to a subclass of initial PNPs as in [2].

Here is an outline of the paper.
In section 2 we first define the circle average by an explicit geometric construction, and then prove that it is indeed an average. For that we prove the *consistency property*, which guarantees that all repeated averages originating from two PNPs can be expressed as one average with an appropriate weight. We also show that the circle average approximates well short pieces of smooth curves, which makes it a good candidate for modifying linear subdivision schemes refining points to schemes refining PNPs, by the approach mentioned above. In section 3 we modify in this way the Lane-Riesenfeld algorithm and also the interpolatory 4-point scheme. We prove that the modified schemes are convergent, and demonstrate by figures and a video their editing capabilities. We provide also a simple method for defining initial normals, in case the input consists of control points only. The advantage of the resulting schemes over the corresponding linear schemes is demonstrated for initial control polygons with edges of significantly different lengths.

## 2 The average

In this section we present the construction of a weighted binary average of two pairs each consisting of a point and a normal. All the weighted averages of the two pairs are located on a circle. When the two pairs are sampled from a circle, the weighted averages stay on that circle.

## 2.1 Construction of the circle average

We first introduce a new binary operation and then show that it is an average, which we term *the circle average*. Given a real weight $\omega \in [0,1]$ and two pairs, each consisting of a point and a normal unit vector $P_0 = (p_0, n_0)$ and $P_1 = (p_1, n_1)$ in $2D$ space, we produce a new pair $P_\omega = (p_\omega, n_\omega)$ denoted by $P_0 \circledcirc_\omega P_1$. For $\omega = \frac{1}{2}$ we use also the shorter notation $P_0 \circledcirc P_1$.

To present the operation $P_0 \circledcirc_\omega P_1$ we introduce some notation. The line defined by the vector $n_i$ and passing through the point $p_i$ is denoted by $l_i, i = 0, 1$. The angle $\theta(u, v)$ denotes the angle between the vectors $u$ and $v$. In the special case of $u = n_0$ and $v = n_1$, the symbol $\theta$ substitutes $\theta(n_0, n_1)$. Observe that $0 \leq \theta \leq \pi$. The length of the segment $[p_0, p_1]$ is denoted by $|p_0p_1|$, and $\overrightarrow{p_0p_1}$ denotes the vector $\overrightarrow{p_1 - p_0}$.

Given three non-collinear points $a, b, c$, we denote by $bc$ the line passing through $b$ and $c$, and by $HP(a; bc)$ the half-plane defined by the line $bc$ which contains the point $a$. For two unit vectors $u = (\cos\alpha, \sin\alpha), v = (\cos\beta, \sin\beta)$, we denote by $GA(u, v; \omega)$ their weighted geodesic average given by

$$GA(u, v; \omega) = (\cos\gamma, \sin\gamma),\ \gamma = (1-\omega)\alpha + \omega\beta. \tag{1}$$

The construction of $P_\omega = \{p_\omega, n_\omega\} = P_0 \circledcirc_\omega P_1$ is done in several steps.

1. Construct the perpendicular $[p_0, p_1]^\perp$ to the segment $[p_0, p_1]$ at its midpoint. Compute the angle $\theta$. Construct two circles with centers $o_0$ and $o_1$ on $[p_0, p_1]^\perp$, passing through $p_0$ and $p_1$, so that the central angles $\sphericalangle p_0 o_i p_1, i = 0, 1$ equal $\theta$. Note that the two circles are symmetric relative to the segment $[p_0, p_1]$, with the same radius $\frac{|p_0p_1|}{2sin\frac{\theta}{2}}$.

2. For each circle, take the short arc connecting $p_0$ and $p_1$. We call the above two arcs "candidate arcs", and the two circles "candidate circles". One of the candidate arcs is chosen in the next step. We denote the selected candidate arc by $\widehat{P_0 \circledcirc P_1}$, its length by $|\widehat{P_0 \circledcirc P_1}|$, and the center of the corresponding circle by $o^*$.

3. **Selection Criterion.** Let $q$ be the intersection point of $l_0$ and $l_1$. Consider the two half-planes defined by the line $p_0p_1$. If $n_0$ and $n_1$ are in different half-planes (relative to $p_0p_1$) then take as $\widehat{P_0 \circledcirc P_1}$ the arc which is in the same half-plane as $q$, otherwise $\widehat{P_0 \circledcirc P_1}$ is the other candidate arc.

4. Compute $p_\omega \in \widehat{P_0 \circledcirc P_1}$ such that the length of the part of $\widehat{P_0 \circledcirc P_1}$ between $p_0$ and $p_\omega$ is $\omega|\widehat{P_0 \circledcirc P_1}|$, or equivalently such that the angle $\sphericalangle p_0 o^* p_\omega = \omega\theta$.

5. Take the normal $n_\omega$ as $GA(n_0, n_1; \omega)$.

See Figure 1 for examples. The selection criterion and the following special cases are chosen to guarantee that the circle average depends continuously on the data.

Special cases:

(i) If $\theta = 0$, i.e. $n_0 = n_1$, then $\widehat{P_0 \circledcirc P_1} = [p_0, p_1]$, $p_\omega = (1-\omega)p_0 + \omega p_1$, and $n_\omega = n_0$.

(ii) In case $\theta = \pi$ the construction is not defined.

(iii) If $n_1 \parallel p_0p_1$ then we consider both normals to be in the same half-plane relative to $p_0p_1$, and $q$ to be in the same half-plane as $n_0$ when $\theta(n_1, \overrightarrow{p_0p_1}) = \pi$, and in the other half-plane when $\theta(n_1, \overrightarrow{p_0p_1}) = 0$. The case $n_0 \parallel p_0p_1$ is dealt with similarly.

(iv) If $|p_0p_1| = 0$, i.e. $p_0 = p_1$, then $p_\omega = p_0$, and $n_\omega$ is computed as in 5.

Note that $P_0 \circledcirc_0 P_1 = P_0$ and $P_0 \circledcirc_1 P_1 = P_1$.

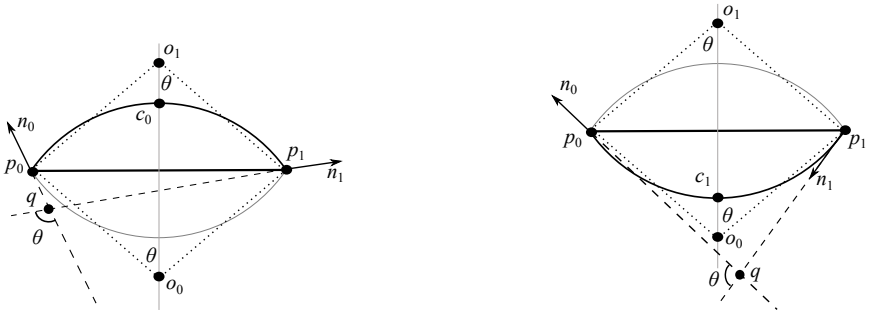


(a) $n_0$ and $n_1$ are in the same half-plane: $p_{\frac{1}{2}} = c_0$.

(b) $n_0$ and $n_1$ are in different half-planes: $p_{\frac{1}{2}} = c_1$.

Figure 1: Construction of $P_0 \circledcirc_{\frac{1}{2}} P_1$.

$\widehat{P_0 \circledcirc P_1}$ is the bold arc.

Two examples of the construction are given in Figure 1. In the left example, the point $c_0$ is taken as the point $p_{\frac{1}{2}}$ since $n_0, n_1 \notin HP(q; p_0p_1)$ and $c_1 \notin HP(q; p_0p_1)$. In the right example, $n_1 \in HP(q; p_0p_1)$ while $n_0 \notin HP(q; p_0p_1)$. Thus the point $c_1 \in HP(q; p_0p_1)$ is selected as $p_{\frac{1}{2}}$. Note that the candidate arcs in both cases are the same, since in both examples $\theta$ is the same.

In the next subsection we show that $P_0 \circledcirc_\omega P_1$ is indeed a weighted average.

## 2.2 The Consistency property

In this section we show that

$$\forall t, s, k \in [0,1], (P_0 \circledcirc_t P_1) \circledcirc_k (P_0 \circledcirc_s P_1) = P_0 \circledcirc_{\omega^*} P_1,\ \omega^* = ks + (1-k)t \quad (2)$$

We call this property of the new operation ***consistency***. With this property the operation $\circledcirc_\omega$ is an average.

To prove (2), we first show

**Lemma 2.1.** Assume w.l.o.g. that $t < s$. Let $P_t = P_0 \circledcirc_t P_1$, and $P_s = P_0 \circledcirc_s P_1$. Then one of the candidate circles for $\widehat{P_t \circledcirc P_s}$ is the same as the circle of $\widehat{P_0 \circledcirc P_1}$.

*Proof.* Let $o^*$ denote the center of the circle of $\widehat{P_0 \circledcirc P_1}$. We show that this circle meets the requirements of a candidate circle for $\widehat{P_t \circledcirc P_s}$. Indeed, it passes

through $p_t$ and $p_s$, and the central angle $\sphericalangle p_t o^* p_s$ equals $(s-t)\theta$, which is the angle between $n_t$ and $n_s$. Thus this circle is a candidate circle for $\widehat{P_t \circledcirc P_s}$. $\square$

Our proof of the consistency property is based upon a classical result in Euclidean geometry.

**Lemma 2.2.** Let $a, b, c, d$ be the four vertices of a convex quadrilateral and let $\sphericalangle a, \sphericalangle b, \sphericalangle c, \sphericalangle d$ be the angles of the quadrilateral at the corresponding vertices. Then

$$\sphericalangle a \geq \pi - \sphericalangle b \iff \pi - \sphericalangle d \geq \sphericalangle c.$$

See Figure 2 for an example.

*Proof.* Since $\sphericalangle a + \sphericalangle b + \sphericalangle c + \sphericalangle d = 2\pi$, $\sphericalangle a + \sphericalangle b \geq \pi \iff \sphericalangle c + \sphericalangle d \leq \pi$, which proves the claim of the lemma. $\square$

The preservation of inequality expressed in Figure 2, follows directly from the lemma.

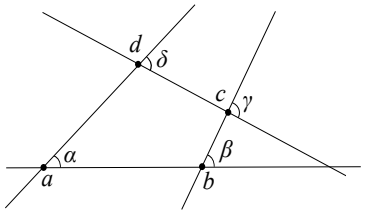


Figure 2: Preserving the inequality $\alpha \leq \beta \Rightarrow \delta \leq \gamma$.

Before proceeding we introduce more notation. Let $P_\omega = P_0 \circledcirc_\omega P_1 = (p_\omega, n_\omega)$. We denote by $l_\omega$ the line through $p_\omega$ in direction $n_\omega$, and by $|\alpha_\omega|$ the angle between the vectors $n_\omega$ and $\overrightarrow{p_0 p_1}$. Note that $0 \leq |\alpha_\omega| \leq \pi$. We introduce the convention that $\alpha_\omega > 0$ ($\alpha_\omega < 0$) if $n_\omega$ is to the left (right) of $\overrightarrow{p_0 p_1}$, when both vectors are anchored in the same point.

We now prove the consistency property in case the two normals are in the same half-plane relative to $p_0 p_1$ or equivalently that $\alpha_0 \alpha_1 > 0$. First, we show

**Theorem 2.3.** *Let $n_0$ and $n_1$ be in the same half-plane relative to $p_0 p_1$, and let $t, s \in [0,1]$, be such that $t < s$. Then,*

$$\widehat{P_t \circledcirc P_s} \subset \widehat{P_0 \circledcirc P_1}\,.$$

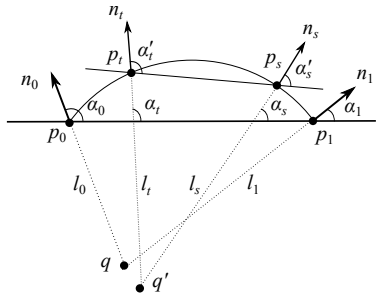


Figure 3: The setup of Theorem 2.3.

*Proof.* W.l.o.g., assume that $\alpha_0 > \alpha_1 > 0$ (see Figure 3). This assumption guarantees that $n_0, n_1 \notin HP(q; p_0p_1)$. Since the vectors $n_0$ and $n_1$ are in the same half-plane relative to $p_0p_1$ the candidate arc in this half-plane is selected by the selection criterion.

According to Lemma 2.1, the circle containing $\widehat{P_0 \circledcirc P_1}$ is considered as a candidate for $\widehat{P_t \circledcirc P_s}$. By definition of $n_t$

$$\alpha_t = (1-t)\alpha_0 + t\alpha_1,\ \alpha_s = (1-s)\alpha_0 + s\alpha_1$$

Since $t < s$ and $\alpha_0 > \alpha_1$, we obtain $\alpha_t > \alpha_s$.
Let $\alpha'_t$ ($\alpha'_s$) be the angle between $p_tp_s$ and $l_t$ ($l_s$), and let $q'$ be the intersection point between $l_t$ and $l_s$. By Lemma 2.2, $\alpha_t > \alpha_s \Rightarrow \alpha'_t > \alpha'_s$. Therefore $n_t, n_s \notin HP(q'; p_tp_s)$, implying that $\widehat{P_t \circledcirc P_s} \subset \widehat{P_0 \circledcirc P_1}$. □

To prove (2) it remains to show that for $P_t \circledcirc_k P_s = (\tilde{p}, \tilde{n})$, $\sphericalangle \tilde{p}o^*p_0 = \omega^*\theta$, and $\theta(n_0, \tilde{n}) = \omega^*\theta$. Indeed

$$\sphericalangle \tilde{p}o^*p_0 = \sphericalangle p_to^*p_0 + k\sphericalangle p_to^*p_s = t\theta + k(s-t)\theta = \omega^*\theta,$$

and similarly

$$\theta(n_0, \tilde{n}) = \theta(n_0, n_t) + k\theta(n_t, n_s) = \omega^*\theta.$$

Next we discuss the case when the normals $n_0, n_1$ are in different half-planes relative to $p_0p_1$.

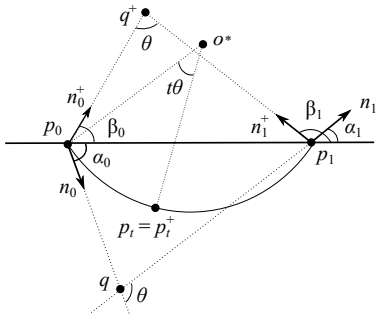


Figure 4: The setup of Theorem 2.4.

**Theorem 2.4.** *For $n_0$ and $n_1$ in different half-planes relative to $p_0p_1$, the consistency, as defined in (2) holds.*

*Proof.* We assume w.l.o.g. that $n_0 \in HP(q; p_0p_1)$ and $n_1 \notin HP(q; p_0p_1)$, namely that $\alpha_0 < 0$, $\alpha_1 > 0$, and that $\pi - |\alpha_0| > \alpha_1$ (see Figure 4).

We take $\beta_0, \beta_1$ such that $0 < \beta_0 < \pi - \theta$, and $\beta_1 = \beta_0 + \theta < \pi$, and define normal vector $n_i^+$ such that $\theta(n_i^+, \overrightarrow{p_0p_1}) = \beta_i$, and a pair $P_i^+ = (p_i, n_i^+)$, for $i = 0, 1$. Note that $\theta(n_0^+, n_1^+) = \theta = \theta(n_0, n_1)$.

Let $q^+$ be the intersection point of the two lines defined for $i = 0, 1$ by the vector $n_i^+$ and passing through the point $p_i$. By the choice of $\beta_0$ and $\beta_1$, we

have $HP(q^+;p_0p_1) \neq HP(q;p_0p_1)$. Thus, according to the selection criterion, $\widehat{P_0^+ \circledcirc P_1^+} = \widehat{P_0 \circledcirc P_1}$.

Let $(p_\omega, n_\omega) = P_0 \circledcirc_\omega P_1$, and $(p_\omega^+, n_\omega^+) = P_0^+ \circledcirc_\omega P_1^+$. By the definition of the average, $\sphericalangle p_0 o^* p_\omega = \omega\theta, \sphericalangle p_0 o^* p_\omega^+ = \omega\theta$, and since $p_\omega$ and $p_\omega^+$ are on $\widehat{P_0 \circledcirc P_1}$, they are equal.

Let $0 < t < s < 1$. By the above discussion $p_t = p_t^+$, $p_s = p_s^+$, while $n_t \neq n_t^+, n_s \neq n_s^+$. By (1), we have

$$\theta(n_t, n_s) = \theta(n_t^+, n_s^+) = (s-t)\theta.$$

Thus, $\widehat{P_t \circledcirc P_s} = \widehat{P_t^+ \circledcirc P_s^+}$, and according to Theorem 2.3

$$\widehat{P_t \circledcirc P_s} = \widehat{P_t^+ \circledcirc P_s^+} \subset \widehat{P_0^+ \circledcirc P_1^+} = \widehat{P_0 \circledcirc P_1}\ .$$

The rest of the proof of (2) is as in the proof of Theorem 2.3. □

Finally, we conclude from Theorem 2.3 and Theorem 2.4,

**Corollary 2.5.** The consistency property holds regardless of the location of the normals relative to $p_0p_1$.

The consistency property of the operation $P_0 \circledcirc_\omega P_1,\ \omega \in [0,1]$ guarantees that it is a weighted binary average and allows to extend it for weights outside [0,1].

Let $\omega^- < 0$ and $\omega^+ > 1$. For $\omega^-$ we extend the arc $\widehat{P_0 \circledcirc P_1}$ on the selected circle outward $p_0$, such that $\sphericalangle p_{\omega^-} o^* p_0 = |\omega^-|\theta$, and similarly, for $\omega^+$ we extend the arc outward $p_1$ such that $\sphericalangle p_{\omega^+} o^* p_0 = \omega^+\theta$. The computation of the normal is done by (1). See Figure 5 for examples.

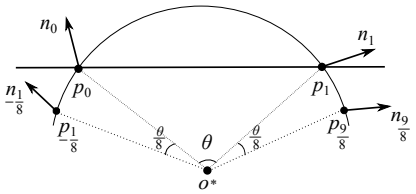


Figure 5: Construction of the circle average with $\omega = -\frac{1}{8}, \frac{9}{8}$.

It is easy to see that this extension is well defined for values of $\omega$ close to [0,1].

## 2.3 The arc $\widehat{P_0 \circledcirc P_1}$ as an approximation tool for curves

In this subsection we compare the quality of the arc $P_0 \circledcirc P_1$ as an approximation tool for curves with that of the optimal arc approximating curves in the least-squares sense. We expect the arc $\widehat{P_0 \circledcirc P_1}$ to approximate well short pieces of smooth curves, in analogy to the approximation capabilities of cubic Hermite interpolation [3, Chapter 6].

Given a parametric curve $\Gamma(t)$, it is sampled at $\{t_i\}_{i=0}^{100}$ with $t_{i+1} - t_i = h > 0$ and also its two normals $n_0$ and $n_{100}$ are sampled at $\Gamma(t_0)$ and $\Gamma(t_{100})$ . We solve the optimization problem of finding the circle $c_{opt}$ minimizing the sum of squares of distances to the input points. Next we construct the arc $a_\Gamma = \widehat{P_0 \circledcirc P_{100}}$, where $P_i = (\Gamma(t_i), n_i)), i = 0, 100$. For every given $\Gamma(t_i)$, we find the nearest point on $c_{opt}$ and on $a_\Gamma$, and measure the distances to these points, denoted by $\rho_i = dist(\Gamma(t_i), c_{opt})$, $\varrho_i = dist(\Gamma(t_i), a_\Gamma)$. The next table presents values of two measures of the quality of the approximation of three analytic curves by $c_{opt}$ and $a_\Gamma$ in two parametric intervals.

| curve | $t_0$ | $t_{100}$ | $\max_{0 \le i \le 100} \rho_i$ | $\max_{0 \le i \le 100} \varrho_i$ | $\frac{1}{101} \sum_{i=0}^{100} \rho_i$ | $\frac{1}{101} \sum_{i=0}^{100} \varrho_i$ |
|---|---|---|---|---|---|---|
| $x(t) = 2\cos t$ | $\frac{5}{8}\pi$ | $\pi$ | 0.04145 | 0.05984 | 0.01315 | 0.02909 |
| $y(t) = \sin t$ | $\frac{12}{16}\pi$ | $\frac{15}{16}\pi$ | 0.00580 | 0.00710 | 0.00193 | 0.00377 |
| $x(t) = t\cos t$ | $\frac{10}{8}\pi$ | $\frac{17}{8}\pi$ | 0.20098 | 0.28437 | 0.06613 | 0.14787 |
| $y(t) = t\sin t$ | $\frac{24}{16}\pi$ | $\frac{31}{16}\pi$ | 0.02337 | 0.02643 | 0.00794 | 0.01530 |
| $x(t) = t^3 - 3t$ | 0 | $\frac{6}{8}\pi$ | 1.46814 | 1.97726 | 0.49597 | 1.02364 |
| $y(t) = t^2 - 1$ | $\frac{3}{16}\pi$ | $\frac{9}{16}\pi$ | 0.25617 | 0.32838 | 0.09297 | 0.17556 |

Table 1: $c_{opt}$ vs. $a_\Gamma$

The examples in Table 1 demonstrate that $\widehat{P_0 \circledcirc P_1}$ can serve as an approximating tool in scenarios when the sampling is expensive and/or when the computation time is critical. Moreover, the quality of the approximation by $\widehat{P_0 \circledcirc P_1}$ increases as the length of the interval of the parameter $t$ decreases. This observation points to the advantage of approximating a curve by piecewise arcs, and to the possibility of using the circle average in subdivision schemes refining point-normal pairs.

# 3 Subdivision schemes with circle averages

In this section we consider subdivision schemes refining point-normal pairs, which are obtained from converging linear subdivision schemes. To obtain these schemes we express the linear schemes in terms of repeated binary averages of points and replace these averages by the circle average. We term the so obtained schemes "Modified schemes".

It is easy to verify that any modified subdivision scheme reconstructs circles, namely, if the initial data is sampled from a circle, the limit of the modified scheme is that circle.

The convergence of the modified schemes is proved in two parts, the convergence of the points and the convergence of the normals. The proof of the convergence of the points is based on the following result:

**Result A** ([11], Theorem 3.6) A subdivision scheme refining points converges for any initial data, if any sequence of control polygons $\left\{\mathcal{P}^j = \{p_i^j : i \in \mathbb{Z}\}\right\}_{j\in\mathbb{N}_0}$ generated by this scheme satisfies

- $e^{j+1} \leq \eta e^j$, $\eta \in (0,1)$, where $e^j$ is the maximal length of an edge in $\mathcal{P}^j$ (contractivity with factor $\eta$).
- $|p_{2i}^{j+1} - p_i^j| \leq ce^j$, with $c > 0$ (safe displacement).

Since our proof of convergence depends on the modified subdivision scheme, it is given after the scheme is presented.

## 3.1 The modified Lane-Riesenfeld (MLR) algorithm

To obtain the first class of subdivision schemes we substitute the arithmetic average by the circle average in the linear Lane-Riesenfeld algorithm (LLR)[13], obtaining the Modified Lane-Riesenfeld (MLR) algorithm, presented in Algorithm 1.

In Figure 6 we present curves generated by the MLR algorithm with $m = 3$ from the same initial data, but with one initial normal changed, demonstrating the editing capabilities of the algorithm. For comparison we depict also the curves generated by the LLR algorithm.

### 3.1.1 Convergence analysis

First we prove the convergence of the points. Our analysis is based on Result A, which gives sufficient conditions for the convergence of a subdivision scheme refining points. These conditions in fact apply to any sequence of control polygons.

First, we introduce some additional notation related to the MLR algorithm. For $k = 0, ..., m-1$ and $j \in \mathbb{N}_0$, $P_i^{j,k} = (p_i^{j,k}, n_i^{j,k})$ and

$$\begin{aligned} e^{j,k} &= \max_{i\in\mathbb{Z}} \{|p_i^{j,k}\ p_{i+1}^{j,k}|\}, \\ \theta^{j,k} &= \max_{i\in\mathbb{Z}} \{\theta(n_i^{j,k}, n_{i+1}^{j,k})\}, \\ \mu^{j,k} &= \frac{1}{2\cos\frac{\theta^{j,k}}{4}}. \end{aligned} \tag{3}$$

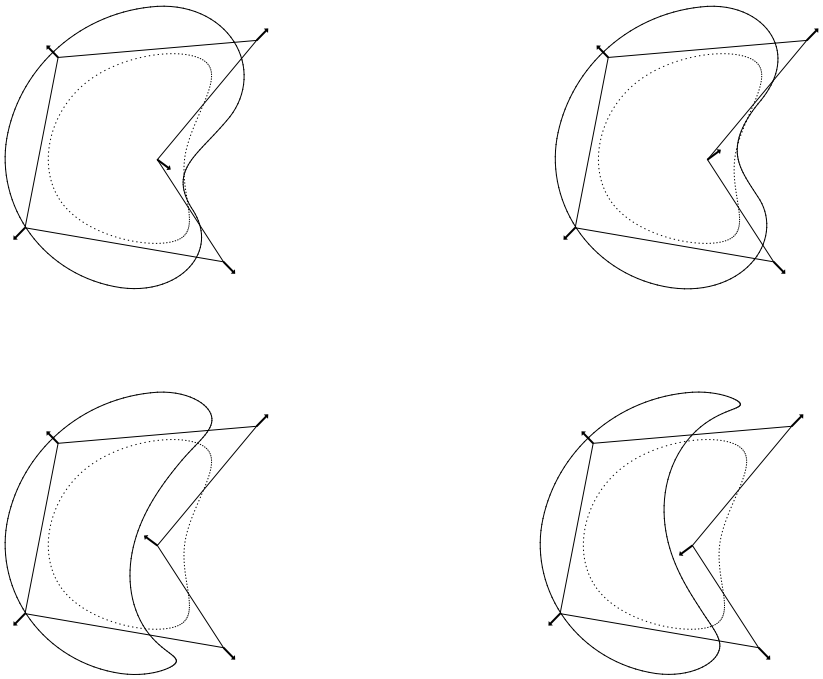

Figure 6: Editing capabilities of the MLR with $m = 3$ by a change of one initial normal.
bold: MLR curve, dots: LLR curve.

**Algorithm 1** MLR

**Input:** $m \in \mathbb{N}_0,\ P_i = (p_i, n_i),\ i \in \mathbb{Z}$.

**for** $i \in \mathbb{Z}$ **do**
  $P_i^0 \leftarrow P_i$
**end for**
**for** j=1,2,... **do**
  **for** $i \in \mathbb{Z}$ **do**
    $P_{2i}^{j,0} \leftarrow P_i^{j-1}$
    $P_{2i+1}^{j,0} \leftarrow P_i^{j-1} \circledcirc_{\frac{1}{2}} P_{i+1}^{j-1}$
  **end for**(i)
  } elementary refinement
  **for** $k = 1, \ldots, m-1$ **do**
    **for** $i \in \mathbb{Z}$ **do**
      $P_i^{j,k} \leftarrow P_i^{j,k-1} \circledcirc_{\frac{1}{2}} P_{i+1}^{j,k-1}$
    **end for**(i)
    } smoothing step
  **end for**(k)
  **for** $i \in \mathbb{Z}$ **do**
    $P_i^j \leftarrow P_i^{j,m-1}$
  **end for**(i)
  } result of current iteration
**end for**(j)

We also define for $j \in \mathbb{N}_0$

$$e^j = e^{j,m-1},\ \theta^j = \theta^{j,m-1},\ \mu^j = \mu^{j,m-1}. \tag{4}$$

Next we prove that the MLR satisfies the first condition of Result A from a certain refinement level and on.

**Lemma 3.1.** There exists $j^* \in \mathbb{N}_0$ such that the MLR algorithm is contractive in refinement levels above $j^*$, namely satisfies $e^{j+1} \leq \eta e^j$ with $\eta \in (0,1)$, for $j \geq j^*$.

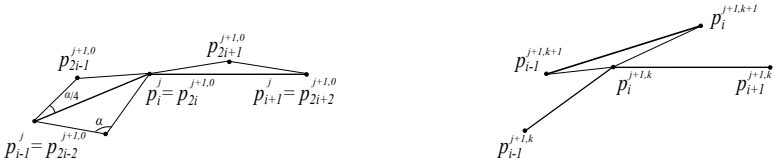


(a) $k = 0$. (b) $k = 1, 2, ..., m-2$.

Figure 7: The setup of Lemmas 3.1 and 3.2

*Proof.* Consider the pairs $\{P_{2i+1}^{j,0}\}_{i\in\mathbb{Z}}$ inserted in the elementary refinement step of the MLR algorithm. By the definition of the circle average (see Figure 7a), we have

$$|p_{2i}^{j+1,0}\ p_{2i+1}^{j+1,0}| = \frac{|p_i^j\ p_{i+1}^j|}{2\cos\left(\frac{\theta(n_i^j, n_{i+1}^j)}{4}\right)} \leq \frac{e^j}{2\cos\left(\frac{\theta^j}{4}\right)} \leq \mu^j e^j. \tag{5}$$

Thus

$$e^{j+1,0} \leq \mu^j e^j. \tag{6}$$

In any smoothing step by the triangle inequality, and similar reasoning leading to (5) (see Figure 7b), we have

$$|p_i^{j,k+1}\ p_{i+1}^{j,k+1}| \leq |p_i^{j,k+1}\ p_{i+1}^{j,k}| + |p_{i+1}^{j,k}\ p_{i+1}^{j,k+1}| \leq \frac{e^{j,k}}{2\cos\left(\frac{\theta^{j,k}}{4}\right)} + \frac{e^{j,k}}{2\cos\left(\frac{\theta^{j,k}}{4}\right)} \leq e^{j,k}\ 2\mu^{j,k}.$$

Therefore

$$e^{j,k+1} \leq e^{j,k}(2\mu^{j,k}),\ k = 0, \ldots, m-2. \tag{7}$$

Combining (7) and (6) we obtain

$$\begin{aligned} e^{j+1} = e^{j+1,m-1} &\leq 2\mu^{j+1,m-2} e^{j+1,m-2} \leq \ldots \\ &\leq (2\mu^{j+1,m-2}) \ldots (2\mu^{j+1,0}) e^{j+1,0} \\ &\leq \left(\mu^j \prod_{k=0}^{m-2} (2\mu^{j+1,k})\right) e^j \end{aligned} \tag{8}$$

Defining $\eta^{j+1} = \mu^j \prod_{k=0}^{m-2} (2\mu^{j+1,k})$ we obtain from (8) and (4)

$$e^{j+1} \leq \eta^{j+1} e^j, \tag{9}$$

with

$$\eta^{j+1} = \prod_{k=0}^{m-2} \left( \frac{1}{\cos \frac{\theta^{j+1,k}}{4}} \right) \frac{1}{2 \cos \frac{\theta^j}{4}} \tag{10}$$

By the subdivision of the normals, we have

$$\theta^{j+1,0} \leq \frac{1}{2}\theta^j, \quad \theta^{j+1,k} \leq \theta^{j+1,k-1}. \tag{11}$$

Thus

$$\theta^{j+1} = \theta^{j+1,m-1} \leq \theta^{j+1,0} \leq \frac{1}{2}\theta^j. \tag{12}$$

In view of (11) and (12) $\theta^{j,k} \leq \theta^{j,0} \leq \theta^{j-1}, k = 0, ..., m-1$, and we get from (10)

$$\eta^{j+1} \leq \frac{1}{2} \left( \frac{1}{\cos \frac{\theta^j}{4}} \right)^m. \tag{13}$$

We also conclude from (12) that $\frac{1}{\cos \frac{\theta^j}{4}}$ is monotone decreasing with $j$.
Let $j^*$ be the minimal $j$ for which

$$\left( \frac{1}{\cos \frac{\theta^j}{4}} \right)^m < 2. \tag{14}$$

Then for $j \geq j^*$, $\eta^j \leq \eta^{j^*} < 1$ and by (9) the MLR is contractive. □

Defining $\theta_m = \theta^{j^*}$ we obtain from (14)

$$\theta_m = 4 \arccos \frac{1}{\sqrt[m]{2}}$$

For $m = 1$, $\theta_1 = 4 \arccos \frac{1}{2} = 4\frac{\pi}{3} > \pi$, and since the angle between any two normal vectors is at most $\pi$, we conclude that the MLR algorithm is contractive for any initial data from the first level. Similarly for $m = 2$, since

$$\theta_2 = 4 \arccos \frac{1}{\sqrt{2}} = 4\frac{\pi}{4} = \pi.$$

For $m = 3$, $\theta_3 = 4 \arccos \frac{1}{\sqrt[3]{2}} > \frac{7}{9}\pi$ and the MLR algorithm with $m = 3$ is contractive from level $j^* = 1$. We give in Table 2 lower bounds of $\theta_m$ for several small values of $m$.

| m | 1 | 2 | 3 | 4 | 5 | 6 |
|---|---|---|---|---|---|---|
| $\theta_m$ | $> \pi$ | $\pi$ | $> \frac{7}{9}\pi$ | $> \frac{13}{18}\pi$ | $> \frac{11}{18}\pi$ | $> \frac{10}{18}\pi$ |

Table 2: $\theta_m$ as a function of $m$

As can be concluded from Table 2, $j^* = 1$ for $3 \le m \le 6$.

To show the convergence of the MLR scheme by Result A, it remains to prove that the scheme is displacement safe.

**Lemma 3.2.** The MLR scheme is displacement safe.

*Proof.* The proof uses the notation of Lemma 3.1 and its proof. By the triangle inequality and since $p_{2i}^{j+1,0} = p_i^j$, $p_{2i}^{j+1} = p_{2i}^{j+1,m-1}$ we get

$$|p_{2i}^{j+1} \; p_i^j| \le \sum_{k=0}^{m-2} |p_{2i}^{j+1,k} p_{2i}^{j+1,k+1}|. \tag{15}$$

In view of Algorithm 1 and the geometry of the circle average (see Figure 7) we have

$$e^{j+1,k+1} \le 2 \max_i |p_i^{j+1,k} \; p_i^{j+1,k+1}|, \;\; k = 0, ..., m-2,$$

$$|p_i^{j+1,k} \; p_i^{j+1,k+1}| \le \frac{e^{j+1,k}}{2\cos\frac{\theta^{j+1,k}}{4}}, \;\; k = 0, ..., m-2,$$

$$e^{j+1,0} \le \frac{e^j}{2\cos\frac{\theta^j}{4}}.$$

Thus for $k = 0, ..., m-2$,

$$\begin{aligned} \max_i |p_i^{j+1,k} \; p_i^{j+1,k+1}| &\le \frac{\max_i |p_i^{j+1,k-1} \; p_i^{j+1,k}|}{\cos\frac{\theta^{j+1,k}}{4}} \le \cdots \le \frac{\max_i |p_i^{j+1,0} \; p_i^{j+1,1}|}{\prod_{h=1}^{k} \cos\frac{\theta^{j+1,h}}{4}} \\ &\le \frac{e^{j+1,0}}{2\cos\frac{\theta^{j+1,0}}{4} \prod_{h=1}^{k} \cos\frac{\theta^{j+1,h}}{4}} \le \frac{e^j}{4\cos\frac{\theta^j}{4} \prod_{h=0}^{k} \cos\frac{\theta^{j+1,h}}{4}} \end{aligned} \tag{16}$$

By (11),(12) and since $\theta^j \le \theta^0 \le \pi$ we have $\frac{\theta^{j+1,k}}{4} \le \frac{\theta^j}{4} < \frac{\pi}{3}$, $k = 0, 1, \ldots, m-1$, and (16) can be replaced by

$$\max_i |p_{2i}^{j+1,k} \; p_{2i}^{j+1,k+1}| \le \frac{e^j}{4\Big(\cos\frac{\pi}{3}\Big)^{k+2}} \le 2^k e^j, \;\; k = 0, 1, \ldots, m-2.$$

Insertion of this bound in (15) leads to

$$\max_i |p_{2i}^{j+1} p_i^j| \le e^j \sum_{k=0}^{m-2} 2^k \le 2^{m-1} e^j.$$

This proves that the MLR scheme is displacement safe, with a constant which grows exponentially with $m$. □

We conclude from Lemmas 3.1, 3.2 and Result A the convergence of the points. It remains to prove the convergence of the normals. Recalling that the operation between the normals in the circle average is a geodesic average independent of the points, the convergence of the normals is a direct consequence of the following result, which is a special case of Corollary 3.3 in [10].

**Result B** ([10], Corollary 3.3) The LR algorithm with the Euclidean average replaced by a geodesic average is convergent.

**Corollary 3.3.** The MLR scheme for $m \geq 1$ is convergent.

### 3.1.2 Interactive demo

We developed an interactive software with drawing capabilities, whose input consists of point-normal pairs, and its output is the corresponding limit of the MLR scheme with $m = 1$, displayed on the screen. In this software points can be dragged, normals can be rotated, and control polygons can be extended and reflected. Also several control polygons can be maintained simultaneously.

As an example, the head of Mickey Mouse is drawn, starting from a simple control polygon. A video of the drawing process, from an empty screen to the final sketch of Mickey Mouse can be found at `https://youtu.be/CGTiDztzVaM`. This example demonstrates the drawing capabilities of the MLR scheme, with $m = 1$, and the quality of naive choice of initial normals, as explained in subsection 3.3.

## 3.2 The modified 4-point scheme (M4Pt)

In this section we modify the interpolatory linear 4-point subdivision scheme (L4Pt) [8],[5],

$$p_{2i}^{j+1} = p_i^j,\ p_{2i+1}^{j+1} = -\frac{1}{16}\big(p_{i-1}^j + p_{i+2}^j\big) + \frac{9}{16}\big(p_i^j + p_{i+1}^j\big) \tag{17}$$

We use the form suggested in [12] for the refinement rule in (17) written in terms of repeated binary averages as

$$p_{2i+1}^{j+1} = \frac{1}{2}\big(\frac{9}{8}p_i^j - \frac{1}{8}p_{i-1}^j\big) + \frac{1}{2}\big(\frac{9}{8}p_{i+1}^j - \frac{1}{8}p_{i+2}^j\big). \tag{18}$$

The modified 4-point scheme (M4Pt) with the circle average replacing the arithmetic average is presented in Algorithm 2.

**Algorithm 2** M4Pt

**Input:** $P_i = (p_i, n_i),\ i \in \mathbb{Z}$.

**for** $i \in \mathbb{Z}$ **do**
  $P_i^0 \leftarrow P_i$
**end for**
**for** j=1,2,... **do**
  **for** $i \in \mathbb{Z}$ **do**
    $P_{2i}^j \leftarrow P_i^{j-1}$
    $S_L \leftarrow P_i^{j-1} \circledcirc_{-\frac{1}{8}} P_{i-1}^{j-1}$
    $S_R \leftarrow P_{i+1}^{j-1} \circledcirc_{-\frac{1}{8}} P_{i+2}^{j-1}$
    $P_{2i+1}^j \leftarrow S_L \circledcirc_{\frac{1}{2}} S_R$
  **end for**
**end for**

Figure 8 demonstrates the editing capabilities of the M4Pt scheme by a change of one initial normal. Note that the control polygon and the normals in this example are the same as those in Figure 6.

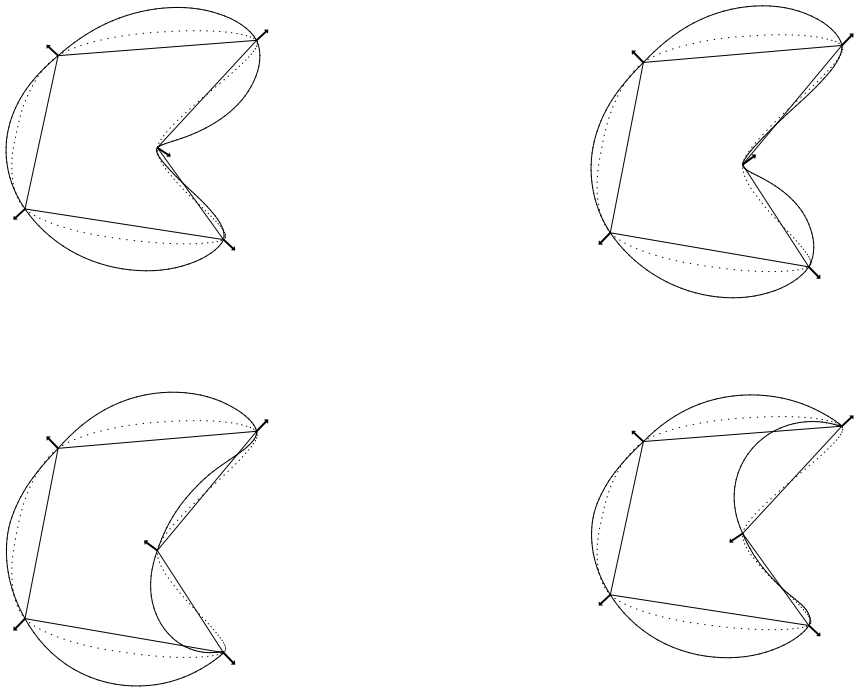

Figure 8: Editing capabilities of the M4Pt by a change of one initial normal. bold: M4Pt curve, dots: L4Pt curve.

### 3.2.1 Convergence analysis

We begin the analysis by proving the convergence of the normals. As we mentioned, the operation between the normals in the circle average is a geodesic average independent of the points. The convergence of the normals is a direct consequence of the following result.

**Result C** ([11], Example 5.1) The 4-point scheme adapted to manifold valued data by replacing in (18) the average by geodesic average is convergent.

By definition, any interpolatory subdivision is displacement safe. Thus it remains to prove the contractivity of the M4Pt, in order to show its convergence by Result A.

**Lemma 3.4.** (Contractivity) The M4Pt scheme is contractive for $j$ large enough.

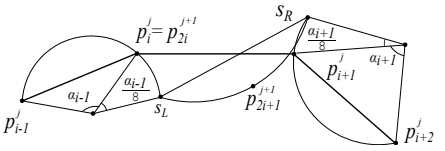


Figure 9: The setup of Lemma 3.4.

*Proof.* Let $S_L = (s_L, n_L),\ S_R = (s_R, n_R)$ be the intermediate pairs obtained by the M4Pt scheme (see Algorithm 2). For the proof we introduce the notation $\alpha_i = \theta(n_i^j, n_{i+1}^j)$. By the triangle inequality and the geometry of the circle average (see Figure 9),

$$|p_{2i}^{j+1}p_{2i+1}^{j+1}| \le |p_{2i+1}^{j+1}s_L| + |s_L p_{2i}^{j+1}| \le \frac{|s_R s_L|}{2\cos(\frac{1}{4}\theta(n_L, n_R))} + \frac{|p_{i-1}^j p_i^j| sin\frac{\alpha_{i-1}}{16}}{sin\frac{\alpha_{i-1}}{2}}. \tag{19}$$

Next we show that

$$\theta(n_L, n_R) \le \frac{5}{4}\theta^j. \tag{20}$$

Indeed, $\theta(n_L, n_R) \le \theta(n_L, n_i^j) + \theta(n_i^j, n_{i+1}^j) + \theta(n_{i+1}^j, n_R)$, where $\theta(n_L, n_i^j) = \frac{1}{8}\theta(n_{i-1}^j, n_i^j)$ and similarly $\theta(n_R, n_{i+1}^j) = \frac{1}{8}\theta(n_{i+1}^j, n_{i+2}^j)$. Since $\theta^j = \max_i \theta(n_i^j, n_{i+1}^j)$, (20) follows.

To bound $|s_L s_R|$ we use again the triangle inequality

$$|s_L s_R| \le |s_L p_i^j| + |p_i^j p_{i+1}^j| + |p_{i+1}^j s_R|,$$

and since $S_L = P_i^j \circledcirc_{-\frac{1}{8}} P_{i-1}^j,\ S_R = P_{i+1}^j \circledcirc_{-\frac{1}{8}} P_{i+2}^j$,

$$|s_L p_i^j| \le \frac{|p_{i-1}^j p_i^j| sin\frac{\alpha_{i-1}}{16}}{sin\frac{\alpha_{i-1}}{2}},\ |s_R p_{i+1}^j| \le \frac{|p_{i+2}^j p_{i+1}^j| sin\frac{\alpha_{i+1}}{16}}{sin\frac{\alpha_{i+1}}{2}} \tag{21}$$

Thus

$$|s_L s_R| \le e^j\Big(1 + \frac{sin\frac{\alpha_{i-1}}{16}}{sin\frac{\alpha_{i-1}}{2}} + \frac{sin\frac{\alpha_{i+1}}{16}}{sin\frac{\alpha_{i+1}}{2}}\Big), \tag{22}$$

and we get from (19), (20) and (22)

$$|p_{2i}^{j+1}p_{2i+1}^{j+1}| \le e^j\Big(1 + \frac{sin\frac{\alpha_{i-1}}{16}}{sin\frac{\alpha_{i-1}}{2}} + \frac{sin\frac{\alpha_{i+1}}{16}}{sin\frac{\alpha_{i+1}}{2}}\Big)\frac{1}{2\cos\frac{5}{16}\theta^j} + e^j\Big(\frac{sin\frac{\alpha_{i-1}}{16}}{sin\frac{\alpha_{i-1}}{2}}\Big).$$

Similarly

$$|p_{2i+1}^{j+1}p_{2i+2}^{j+1}| \le e^j\Big(1 + \frac{sin\frac{\alpha_{i-1}}{16}}{sin\frac{\alpha_{i-1}}{2}} + \frac{sin\frac{\alpha_{i+1}}{16}}{sin\frac{\alpha_{i+1}}{2}}\Big)\frac{1}{2\cos\frac{5}{16}\theta^j} + e^j\Big(\frac{sin\frac{\alpha_{i+1}}{16}}{sin\frac{\alpha_{i+1}}{2}}\Big).$$

Therefore

$$e^{j+1} \le e^j\Big(1 + \frac{sin\frac{\alpha_{i-1}}{16}}{sin\frac{\alpha_{i-1}}{2}} + \frac{sin\frac{\alpha_{i+1}}{16}}{sin\frac{\alpha_{i+1}}{2}}\Big)\frac{1}{2\cos\frac{5}{16}\theta^j} + Ae^j,$$

with

$$A = \max_i \frac{sin\frac{\alpha_i}{16}}{sin\frac{\alpha_i}{2}}.$$

Thus, $e^{j+1} \leq \eta^j e^j$ with

$$\eta^j = \frac{1}{2}\Big(1 + \frac{sin\frac{\alpha_{i-1}}{16}}{sin\frac{\alpha_{i-1}}{2}} + \frac{sin\frac{\alpha_{i+1}}{16}}{sin\frac{\alpha_{i+1}}{2}}\Big)\frac{1}{\cos\frac{5}{16}\theta^j} + A. \tag{23}$$

Since $\alpha_i \leq \theta^j$ and the normals converge, $\lim_{j\to\infty} \theta^j = 0$. Thus we get from (23)

$$\eta^* = \lim_{j\to\infty} \eta^j = \frac{1}{2}(1 + \frac{1}{8} + \frac{1}{8}) + \frac{1}{8} = \frac{3}{4} \tag{24}$$

We conclude from (24) that for $j$ large enough $\eta^j < 1$. Defining $J^*$ such that $\eta^j < \frac{7}{8}$ for $j \geq J^*$, we get that the M4Pt scheme is contractive for $j \geq J^*$, with $\eta^j = \frac{7}{8}$. □

We conclude from Lemma 3.4 and Result A the convergence of the points.

**Corollary 3.5.** The M4Pt scheme is convergent.

## 3.3 Naive choice of initial normals

In previous sections we discussed the scenario in which normals are given at every vertex of the input control polygon. In this section we propose a method for determining initial normals at the vertices of a given control polygon.

To determine a normal at the vertex $p_i$, we first compute the normals $v_{i-1}, v_i$ to the neighboring edges of the vertex $p_i$, and the length of these edges, $d_{i-1}, d_i$. We chose the direction of $v_i$, the normal to the edge $p_ip_{i+1}$, such that $v_i \times \overrightarrow{p_ip_{i+1}} > 0$. The normal at $p_i$ is the weighted geodesic average of $v_{i-1}, v_i$ as defined in (1), with weights proportional to the reciprocal of the length of the corresponding edge,

$$n_i = GA\Big(v_{i-1}, v_i; \frac{d_{i-1}}{d_i + d_{i-1}}\Big).$$

In case $p_i$ is a boundary vertex, the normal is taken as that of the only neighboring edge.

Figure 10 depicts a control polygon and different curves obtained from it by two modified schemes with initial normals computed by the "naive method". For comparison the curves generated by the corresponding linear schemes from the same initial control polygon are also shown. Figure 10a demonstrates that the MLR algorithm with $m = 3$ preserves the shape of the control polygon more accurately than the corresponding LLR scheme. In Figure 10b we see that the L4Pt scheme generates a self intersecting curve while the curve of the M4Pt scheme is self intersection free and follows the shape of the initial polygon smoothly.

The proposed "naive method" determines intuitive initial normals, which can be modified later on, as is shown in the example of subsection 3.1.2.

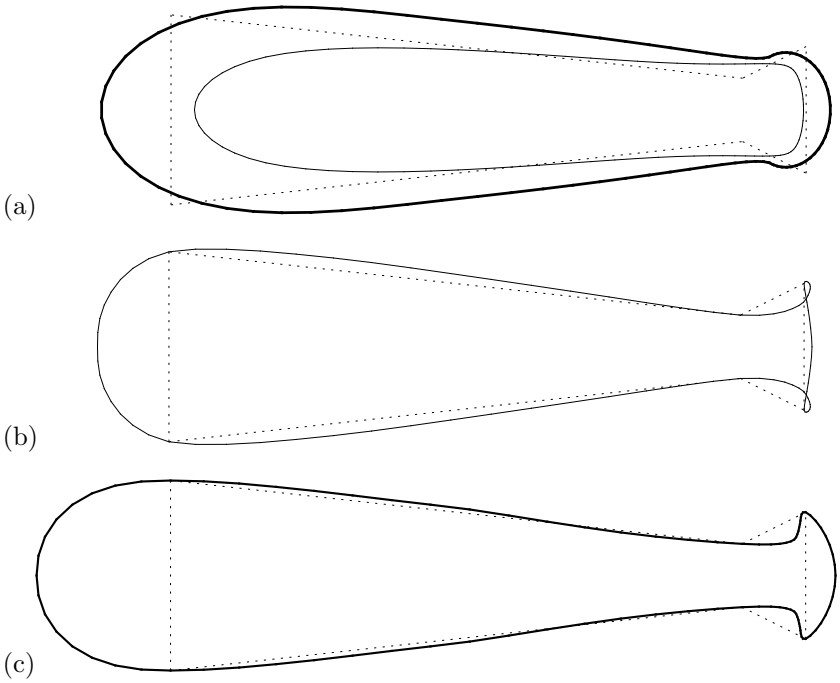


Figure 10: Comparison between modified schemes and their corresponding linear schemes. Same initial control polygon (dots); (a)MLR (bold) and LLR (regular); (b)L4Pt; (c) M4Pt.

## Acknowledgment

The authors thank Prof. D. Cohen-Or for fruitful discussions, and the reviewers for their valuable comments. This work was partially supported by Minkowski Minerva center at Tel-Aviv University.

## References

[1] Thomas J. Cashman, Kai Hormann, and Ulrich Reif. Generalized Lane-Riesenfeld algorithms. *Computer Aided Geometric Design*, 30(4), 2013.

[2] Pavel Chalmovianský and Bert Jüttler. A non–linear circle–preserving subdivision scheme. *Adv. Comp. Math.*, 27:375–400, 2007.

[3] Samuel Daniel Conte and Carl W. De Boor. *Elementary Numerical Analysis: An Algorithmic Approach*. McGraw-Hill Higher Education, 3rd edition, 1980.

[4] Costanca Conti and Nira Dyn. Analysis of subdivision schemes for nets of functions by proximity and controllability. *Journal of Computational and Applied Math*, 236:461–475, 2011.

[5] Gilles Deslauriers and Serge Dubuc. Symmetric iterative interpolation processes. *Constractive Approximation.*, 5(1):49–68, 1989. Fractal approximation.

[6] Neil A. Dodgson and Malcolm A. Sabin. A circle-preserving variant of the four-point scheme. *Mathematical Methods for Curves and Surfaces: Tromso 2004*, pages 275–286, 2005.

[7] Nira Dyn and Elza Farkhi. Spline subdivision schemes for compact sets-a survey. *Serdica Math. J.*, 28 (4):349–360, 2002.

[8] Nira Dyn, John A. Gregory, and David Levin. A 4-point interpolatory subdivision scheme for curve design. *Comput. Aided Geom. Design*, 4(4):257–268, 1987.

[9] Nira Dyn and David Levin. Subdivision schemes in geometric modelling. *Acta Numerica*.

[10] Nira Dyn and Nir Sharon. A global approach to the refinement of manifold data. *Mathematics of Computation*, 1:1–2, 2016.

[11] Nira Dyn and Nir Sharon. Manifold-valued subdivision schemes based on geodesic inductive averaging. *Journal of Computational and Applied Mathematics*, 2016.

[12] Shay Kels and Nira Dyn. Subdivision schemes of sets and the approximation of set-valued functions in the symmetric difference metric. *Foundations of Computational Mathematics*, 13(5):835–865, 2013.

[13] Jeffrey M. Lane and Richard F. Riesenfeld. A theoretical development for the computer generation and display of piecewise polynomial surfaces. *IEEE Transactions on Pattern Analysis and Machine Intelligence*, PAMI-2(1):35–46, 1980.

[14] Jean-Louis Merrien. A family of hermite interpolants by bisection algorithms. *Numerical Algorithms*, 2:187–200, June 1992.

[15] Inam Ur Rahman, Iddo Drori, Victoria C. Stodden, David L. Donoho, and Peter Schröder. Multiscale representations for manifold-valued data. *Multiscale Model. Simul.*, 4(4):1201–1232, 2005.

[16] Johannes Wallner and Nira Dyn. Convergence and $C^1$ analysis of subdivision schemes on manifolds by proximity. *Computer Aided Geometric Design*, 22(7):593–622, 2005.